

Relevance of electron-lattice coupling in cuprates superconductors

T. Schneider¹, R. Khasanov^{1,2}, K. Conder³, and H. Keller¹

⁽¹⁾ *Physik-Institut der Universität Zürich, Winterthurerstrasse 190, CH-8057, Switzerland*

⁽²⁾ *Paul Scherrer Institut, Labor für Myon-Spin Spektroskopie, CH-5232 Villigen PSI, Switzerland*

⁽³⁾ *Laboratory for Neutron Scattering, ETH Zürich and PSI Villigen, CH-5232 Villigen PSI, Switzerland*

We study the oxygen isotope (¹⁶O,¹⁸O) and finite size effects in $Y_{1-x}Pr_xBa_2Cu_3O_{7-\delta}$ by in-plane penetration depth (λ_{ab}) measurements. A significant change of the length L_c of the superconducting domains along the c -axis and λ_{ab}^2 is deduced, yielding the relative isotope shift $\Delta L_c/L_c \approx \Delta\lambda_{ab}^2/\lambda_{ab}^2 \approx -0.14$ for $x = 0, 0.2$ and 0.3 . This uncovers the existence and relevance of the coupling between the superfluid, lattice distortions and anharmonic phonons which involve the oxygen lattice degrees of freedom.

PACS numbers: 74.72.Bk, 74.25.Kc, 74.62.Yb

Since the discovery of superconductivity in cuprates by Bednorz and Müller[1] a tremendous amount of work has been devoted to their characterization. The issue of inhomogeneity and its characterization is essential for several reasons, including: First, if inhomogeneity is an intrinsic property, a re-interpretation of experiments, measuring an average of the electronic properties, is unavoidable. Second, inhomogeneity may point to a microscopic phase separation, i.e. superconducting domains, embedded in a nonsuperconducting matrix. Third, there is neutron spectroscopic evidence for nanoscale cluster formation and percolative superconductivity in various cuprates[2, 3]. Fourth, nanoscale spatial variations in the electronic characteristics have been observed in underdoped $Bi_2Sr_2CaCu_2O_{8+\delta}$ with scanning tunnelling microscopy (STM)[4, 5, 6, 7]. They reveal a spatial segregation of the electronic structure into 3nm diameter superconducting domains in an electronically distinct background. On the contrary, a large degree of homogeneity has been observed by Renner and Fischer[8]. As STM is a surface probe the relevance of these observations for bulk and thermodynamic properties remains to be clarified. Fifth, in $YBa_2Cu_3O_{7-\delta}$, MgB_2 , $2H-NbSe_2$ and $Nb_{77}Zr_{23}$ considerably larger domains have been established. The magnetic field induced finite size effect revealed lower bounds ranging from $L = 182$ to 814\AA [9, 10]. Sixth, since the change of the lattice parameters upon oxygen isotope exchange is negligibly small[11, 12], the occurrence of a significant modification of the domains spatial extent, will provide clear evidence for superconductivity mediated by local lattice distortions.

This letter concentrates on $Y_{1-x}Pr_xBa_2Cu_3O_{7-\delta}$ with ¹⁶O and ¹⁸O. It addresses these issues by providing clear evidence for a finite size effect on the in-plane London penetration depth, revealing the existence of superconducting domains with spatial nanoscale extent and its significant change upon oxygen isotope exchange.

Polycrystalline samples of $Y_{1-x}Pr_xBa_2Cu_3O_{7-\delta}$ ($x = 0, 0.2, 0.3$) were synthesized by solid-state reactions [13] and their phase-purity was examined using powder x-ray diffraction. For each doping concentration the sam-

ples were reground in a mortar for about 60min. Powder samples with a grain size of $< 10\mu\text{m}$ were obtained by using a system of $20/15/10\mu\text{m}$ sieves. Oxygen isotope exchange was performed by heating the powder in ¹⁸O₂ gas. In order to ensure the same thermal history of the substituted (¹⁸O) and not substituted (¹⁶O) samples, two experiments (in ¹⁶O₂ and ¹⁸O₂) were always performed simultaneously [13]. To achieve complete oxidation the exchange processes were carried out at 550°C during 30 h, followed by slow cooling ($20^\circ\text{C}/\text{h}$). The ¹⁸O content, determined from a change of the sample weight after the isotope exchange, was found to be 89(2)% for all samples. Field-cooled (FC) magnetization measurements were performed with a Quantum Design SQUID magnetometer in field range 0.5 to 10mT and a temperature range 5K to 100K. The powder samples ($\sim 100\text{mg}$) were put in a quartz ampule. To guarantee the same experimental conditions (sample geometry and the background signal from the sample holder), the same ampule was used. The absence of weak links between grains was confirmed by the linear scaling of the FC magnetization measured at 5K in 0.5mT, 1mT and 1.5mT. The Meissner fraction f was calculated from the mass and the x-ray density, assuming spherical grains. An example of f versus T is displayed in the insert of Fig.1. Assuming spherical grains of radius R , the data were analyzed on the basis of the Shoenberg formula [14], allowing to calculate the temperature dependence of the effective penetration depth $\lambda_{eff}(T)/\lambda_{eff}(0)$. For sufficiently anisotropic extreme type II superconductors, including $Y_{1-x}Pr_xBa_2Cu_3O_{7-\delta}$, λ_{eff} is proportional to the in-plane penetration depth, so that $\lambda_{eff} = 1.31\lambda_{ab}$ [15, 16]. Since it is not possible to extract the absolute value of λ_{ab} from our measurements we take $\lambda_{ab}(0K)$ from μSR measurements[17] to normalize the data. In the main panel of Fig.1 we displayed the resulting temperature dependence of $^{16}\lambda_{ab}^2(0)/\lambda_{ab}^2(T)$ for the ¹⁶O and ¹⁸O samples of $Y_{0.7}Pr_{0.3}Ba_2Cu_3O_{7-\delta}$. For comparison we included $^{16}\lambda_{ab}^2(0)/\lambda_{ab}^2(T) = ^{16}\lambda_{ab}^2(0)/\lambda_{0,ab}^2(1 - T/T_c)^\nu$ with the critical exponent $\nu = 2/3$, $^{16}T_c = 54.9K$ and $^{18}T_c = 53.7K$ to indicate the asymptotic critical behav-

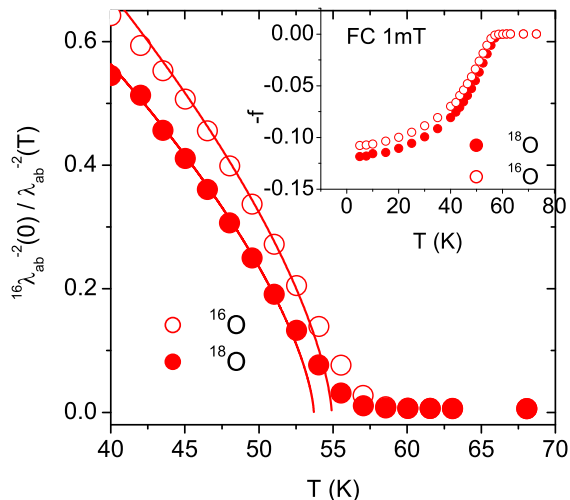


FIG. 1: $(^{16}\lambda_{ab}(0)/\lambda_{ab}(T))^2$ versus T for the ^{16}O and ^{18}O samples of $\text{Y}_{0.7}\text{Pr}_{0.3}\text{Ba}_2\text{Cu}_3\text{O}_{7-\delta}$. The solid lines indicate the leading critical behavior of the homogeneous systems as explained in the text. Inset: Meissner fraction f versus temperature (FC 1mT). The error bars are smaller than the size of the data points.

ior for an infinite superconducting domain. Apparently, the data are inconsistent with such a sharp transition. It clearly uncovers a rounded phase transition which occurs smoothly and with that a finite size effect at work. In this context it is important to emphasize that this finite size effect is not an artefact of $\text{Y}_{1-x}\text{Pr}_x\text{Ba}_2\text{Cu}_3\text{O}_{7-\delta}$ or the particular technique used to evaluate $1/\lambda_{ab}^2(T)$. Indeed, this rounding is also seen in the data for $\text{YBa}_2\text{Cu}_3\text{O}_7$ [18], $\text{La}_{2-x}\text{Sr}_x\text{CuO}_4$ with $x=0.1, 0.15$ and 0.2 [19], and $\text{Bi}_2\text{Sr}_2\text{CaCu}_2\text{O}_{8+\delta}$ single crystals[20, 21]. Moreover, independent evidence for superconducting domains of finite extent, stems from the analysis of specific heat data[10]. Given the mounting evidence for these domains, their behavior upon oxygen isotope exchange is expected to offer valuable clues on the relevance of local lattice distortions in the mechanism mediating superconductivity.

To elucidate this issue we perform a finite size scaling analysis of the in-plane penetration depth data for $\text{Y}_{1-x}\text{Pr}_x\text{Ba}_2\text{Cu}_3\text{O}_{7-\delta}$ with ^{16}O and ^{18}O . Supposing that cuprate superconductors are granular, consisting of spatial superconducting domains, embedded in a non-superconducting matrix and with spatial extent L_a , L_b and L_c along the crystallographic a , b and c -axes, the correlation length ξ_i in direction i , increasing strongly when T_c is approached cannot grow beyond L_i . Consequently, for finite superconducting domains, the thermodynamic quantities like the specific heat and penetration depth are smooth functions of temperature. As a remnant of the singularity at T_c these quantities exhibit a so called finite size effect[22], namely a maximum or an inflection

point at T_{p_i} , where $\xi_i(T_{p_i}) = L_i$. There is mounting experimental evidence that for the accessible temperature ranges, the effective finite temperature critical behavior of the cuprates is controlled by the critical point of uncharged superfluids (3D-XY)[9, 21]. In this case there is the universal relationship

$$\frac{1}{\lambda_i^2(T)} = \frac{16\pi^3 k_B T}{\Phi_0^2 \xi_i^t(T)}, \quad (1)$$

between the London penetration depth λ_i and the transverse correlation length ξ_i^t in direction i [9, 23]. As aforementioned, when the superconductor is inhomogeneous, consisting of superconducting domains with length scales L_i , embedded in a non-superconducting matrix, the ξ_i^t 's do not diverge but are bounded by

$$\xi_i^t \xi_j^t \leq L_k^2, \quad i \neq j \neq k. \quad (2)$$

A characteristic feature of the resulting finite size effect is the occurrence of an inflection point at T_{p_k} below T_c , the transition temperature of the homogeneous system. Here

$$\xi_i^t(T_{p_k}) \xi_j^t(T_{p_k}) = L_k^2, \quad i \neq j \neq k, \quad (3)$$

and Eq.(1) reduces to

$$\frac{1}{\lambda_i(T) \lambda_j(T)} \Big|_{T=T_{p_k}} = \frac{16\pi^3 k_B T_{p_k}}{\Phi_0^2} \frac{1}{L_k}. \quad (4)$$

In the homogeneous case $1/(\lambda_i(T) \lambda_j(T))$ decreases continuously with increasing temperature and vanishes at T_c , while for superconducting domains, embedded in a non-superconducting matrix, it does not vanish and exhibits an inflection point at $T_{p_k} < T_c$, so that

$$d \left(\frac{1}{\lambda_i(T) \lambda_j(T)} \right) / dT \Big|_{T=T_{p_k}} = \text{extremum} \quad (5)$$

We are now prepared to perform the finite size scaling analysis of the penetration depth data. In Fig.2 we displayed $^{16}\lambda_{ab}^2(T=0)/\lambda_{ab}^2(T)$ and $d(^{16}\lambda_{ab}^2(T=0)/\lambda_{ab}^2(T))/dT$ versus T for $\text{Y}_{0.7}\text{Pr}_{0.3}\text{Ba}_2\text{Cu}_3\text{O}_{7-\delta}$. The solid lines are $(^{16}\lambda_{ab}(0)/^{16}\lambda_{ab}(T))^2 = 1.62(1 - T/^{16}T_c)^\nu$, $(^{16}\lambda_{ab}(0)/^{18}\lambda_{ab}(T))^2 = 1.4(1 - T/^{18}T_c)^\nu$ with $\nu = 2/3$, $^{16}T_c = 54.9\text{K}$, $^{18}T_c = 53.7\text{K}$ and the dash dot lines the corresponding derivatives, indicating the leading critical behavior of a domain, infinite in the c -direction. The extreme in the first derivative around $T \approx 52.1\text{K}$ and 51K for ^{16}O and ^{18}O respectively clearly reveal the existence of an inflection point, characterizing the occurrence of a finite size effect in $1/\lambda_{ab}^2$ (Eq.(5)). Using Eq.(4) and the estimates for T_{p_c} , $^{16}\lambda_{ab}^2(T_{p_c})/^{16}\lambda_{ab}^2(0)$, $^{18}\lambda_{ab}^2(T_{p_c})/^{18}\lambda_{ab}^2(0)$ and $^{16}\lambda_{ab}(0)$ listed in Table I, we obtain $^{16}L_c = 19.5(8)\text{\AA}$

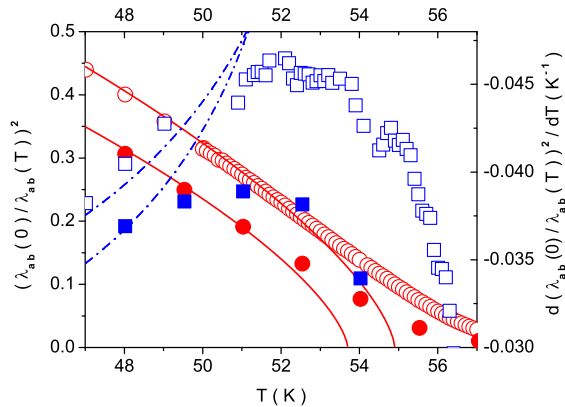


FIG. 2: $^{16}\lambda_{ab}^2(T=0)/\lambda_{ab}^2(T)$ (\circ : ^{16}O , \bullet : ^{18}O) and $d(\lambda_{ab}^2(T=0)/\lambda_{ab}^2(T))/dT$ (\square : ^{16}O , \blacksquare : ^{18}O) versus T for $\text{Y}_{0.7}\text{Pr}_{0.3}\text{Ba}_2\text{Cu}_3\text{O}_7$ with ^{16}O and ^{18}O . The solid and dash dot lines indicate the leading critical behavior of the homogeneous system as explained in the text.

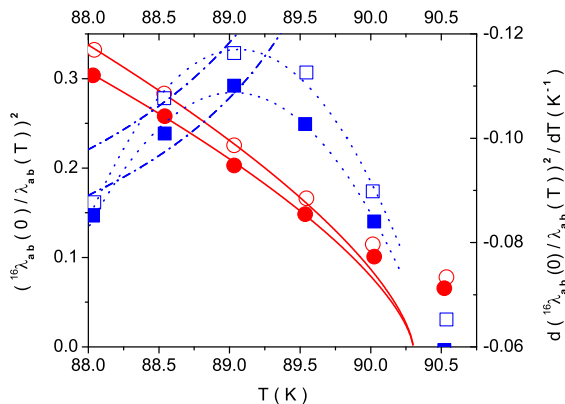


FIG. 3: $^{16}\lambda_{ab}^2(T=0)/\lambda_{ab}^2(T)$ (\circ : ^{16}O , \bullet : ^{18}O) and $d(\lambda_{ab}^2(T=0)/\lambda_{ab}^2(T))/dT$ (\square : ^{16}O , \blacksquare : ^{18}O) versus T for $\text{YBa}_2\text{Cu}_3\text{O}_7$ with ^{16}O and ^{18}O . The solid and dash dot lines indicate the leading critical behavior of the homogeneous system as explained in the text. The dot lines are quadratic fits used to determine the inflection points T_{pc} .

and $^{18}L_c = 22.6(9)\text{\AA}$ for the spatial extent of the superconducting domains along the c -axis. Note that the rather broad peak around the inflection point reflects the small value of L_c . Indeed, in $\text{Bi}2212$, where the same analysis gives $L_c \approx 68\text{\AA}$, this peak was found to be considerably sharper[24].

To explore the dependence of this change on Pr concentration we performed analogous magnetization measurements on $\text{Y}_{1-x}\text{Pr}_x\text{Ba}_2\text{Cu}_3\text{O}_{7-\delta}$ with $x = 0$

and $x = 0.2$ and extracted the in-plane penetration depth, as outlined above. In Fig.3 we show $^{16}\lambda_{ab}^2(T=0)/\lambda_{ab}^2(T)$ and $d(\lambda_{ab}^2(T=0)/\lambda_{ab}^2(T))/dT$ versus T for $\text{YBa}_2\text{Cu}_3\text{O}_{7-\delta}$ with ^{16}O and ^{18}O . The solid lines are $(^{16}\lambda_{ab}(0)/^{16}\lambda_{ab}(T))^2 = 3.9(1 - T/^{16}T_c)^{2/3}$, $(^{16}\lambda_{ab}(0)/^{18}\lambda_{ab}(T))^2 = 3.55(1 - T/^{18}T_c)^{2/3}$ with $^{16}T_c \approx ^{18}T_c = 90.3\text{K}$ and the dash dot lines the corresponding derivatives, indicating the leading critical behavior of the homogeneous system. The finite size estimates for various quantities and the corresponding isotope shifts, for an ^{18}O content 89% are summarized in Table I (we define the relative oxygen isotope shift of a physical quantity X as $\Delta X/X = (^{18}X - ^{16}X)/^{16}X$). While the isotope effect on T_c and the inflection points T_{pc} is very small, there is an appreciable shift of $1/\lambda_{ab}^2$. As indicated in Fig.3, we used a quadratic fit around the inflection point to determine T_{pc} . Nevertheless, the error left (0.1 to 0.2K) leads to the main uncertainty in terms of $\lambda_{ab}^2(T_{pc})/\lambda_{ab}^2(0)$. From Table I several observations emerge. First, L_c increases systematically with reduced T_{pc} . Second, L_c grows with increasing x and upon isotope exchange (^{16}O , ^{18}O). Third, the relative shift of T_{pc} is very small. This reflects the fact that the change of L_c is essentially due to the superfluid, probed in terms of λ_{ab}^2 . Accordingly, $\Delta L_c/L_c \approx \Delta\lambda_{ab}^2/\lambda_{ab}^2$ for $x = 0, 0.2$ and 0.3 . Indeed the relative shifts of T_{pc} , $\lambda_{ab}^2(T_{pc})$ and L_c are not independent. Eq.(4) implies,

$$\frac{\Delta L_c}{L_c} = \frac{\Delta T_{pc}}{T_{pc}} + \frac{\Delta\lambda_{ab}^2(T_{pc})}{\lambda_{ab}^2(T_{pc})}. \quad (6)$$

x	0	0.2	0.3
$\Delta T_{pc}/T_{pc}$	-0.000(2)	-0.015(3)	-0.021(5)
$\Delta L_{pc}/L_{pc}$	0.12(5)	0.13(6)	0.16(5)
$\Delta\lambda_{ab}^2(T_{pc})/\lambda_{ab}^2(T_{pc})$	0.11(5)	0.15(6)	0.15(5)
$^{16}\lambda_{ab}^2(^{16}T_{pc})/^{16}\lambda_{ab}^2(0)$	4.4(2)	4.0(2)	4.4(2)
$^{18}\lambda_{ab}^2(^{18}T_{pc})/^{16}\lambda_{ab}^2(0)$	4.9(2)	4.6(2)	5.2(2)
$^{16}T_{pc}$ (K)	89.0(1)	67.0(1)	52.1(2)
$^{18}T_{pc}$ (K)	89.0(1)	66.0(2)	51.0(2)
$^{16}L_{pc}$ (Å)	9.7(4)	14.2(7)	19.5(8)
$^{18}L_{pc}$ (Å)	10.9(4)	16.0(7)	22.6(9)
$^{16}\lambda_{ab}(0)$ (Å)	1250(10)	1820(20)	2310(30)

Table I: Finite size estimates for $^{16}T_{pc}$, $^{18}T_{pc}$, $\Delta T_{pc} = ^{16}T_{pc} - ^{18}T_{pc}$, $^{16}\lambda_{ab}^2(^{16}T_{pc})/^{16}\lambda_{ab}^2(0)$ and $^{18}\lambda_{ab}^2(^{18}T_{pc})/^{16}\lambda_{ab}^2(0)$, and the resulting relative shifts $\Delta T_{pc}/^{16}T_{pc}$ and $\Delta\lambda_{ab}^2/^{16}\lambda_{ab}^2(^{16}T_{pc})$ for an ^{18}O content of 89%. $^{16}L_{pc}$, $^{18}L_{pc}$ and $\Delta L_{pc}/^{16}L_{pc}$ follow then via Eq.(4). $^{16}\lambda_{ab}(0)$ are μSR estimates[17]

To appreciate the implications of these estimates, we note that for fixed Pr concentration the lattice parameters remain essentially unaffected[11, 12]. Accordingly,

an electronic mechanism, without coupling to local lattice distortions and anharmonic phonons, implies $\Delta L_c = 0$. On the contrary, a significant change of L_{p_c} upon oxygen exchange uncovers the coupling to local lattice distortions and anharmonic phonons involving the oxygen lattice degrees of freedom. A glance to Table I shows that the relative change of the domains along the c-axis upon oxygen isotope exchange is significant, ranging from 12 to 16%, while the relative change of the inflection point or the transition temperature is an order of magnitude smaller. For this reason the significant relative change of L_c at fixed Pr concentration is accompanied by essentially the same relative change of λ_{ab}^2 , which probes the superfluid. This uncovers unambiguously the existence and relevance of the coupling between the superfluid, lattice distortions and anharmonic phonons involving the oxygen lattice degrees of freedom. Potential candidates are the Cu-O bond-stretching-type phonons showing temperature dependence, which parallels that of the superconductive order parameter[25]. Independent evidence for the shrinkage of limiting length scales upon isotope exchange stems from the behavior close to the quantum superconductor to insulator transition where T_c vanishes[26]. Here the cuprates become essentially two dimensional and correspond to a stack of independent slabs of thickness d_s [27, 28]. It was found that the relative shift $\Delta d_s/d_s$ upon isotope exchange adopts a rather unique value, namely $\Delta d_s/d_s \approx -0.03$ [26].

In conclusion, we reported the first observation of the combined finite size and oxygen isotope exchange effects on the spatial extent L_c of the superconducting domains along the c-axis and the in-plane penetration depth λ_{ab} . Although the majority opinion on the mechanism of superconductivity in the cuprates is that it occurs via a purely electronic mechanism involving spin excitations, and lattice degrees of freedom are supposed to be irrelevant, we have shown the relative isotope shift $\Delta L_c/^{16}L_c \approx \Delta \lambda_{ab}^2/^{16}\lambda_{ab}^2 \approx -0.15$ uncovers clearly the existence and relevance of the coupling between the superfluid, lattice distortions and anharmonic phonons which involve the oxygen lattice degrees of freedom.

The authors are grateful to K.A. Müller and J. Roos for very useful comments and suggestions on the subject matter. This work was partially supported by the Swiss National Science Foundation.

-
- [1] G. Bednorz and K. A. Müller, Z. Phys. B **64**, 189 (1986).
 - [2] J. Mesot, P. Allensbach, U. Staub, and A. Furrer, Phys. Rev. Lett. **70**, 865 (1993).
 - [3] A. Furrer *et al.*, Physica C **235-240**, 261 (1994).
 - [4] J. Liu, J. Wan, A. Goldman, Y. Chang, and P. Jiang, Phys. Rev. Lett. **67**, 2195 (1991).
 - [5] A. Chang, Z. Rong, Y. Ivanchenko, F. Lu, and E. Wolf, Phys. Rev. B **46**, 5692 (1992).
 - [6] T. Cren *et al.*, Phys. Rev. Lett. **84**, 147 (2000).
 - [7] K. M. Lang *et al.*, Nature **415**, 413 (2002).
 - [8] Ch. Renner and Ø. Fischer, Phys. Rev. B **51**, 9208 (1995).
 - [9] T. Schneider and J. M. Singer, *Phase Transition Approach To High Temperature Superconductivity* (Imperial College Press, London, 2000).
 - [10] T. Schneider, cond-mat/0210702.
 - [11] K. Conder *et al.*, in *Phase Separation in Cuprate Superconductors*, edited by E. Sigmund and K.A. Müller (Springer, Berlin 1994) p. 210.
 - [12] F. Raffa *et al.*, Phys. Rev. Lett. **81**, 5912 (1998).
 - [13] K. Conder, Mater. Sci. Eng., **R 32**, 41-102 (2001).
 - [14] D. Shoenberg, *Superconductivity* (Cambridge University, Cambridge, 1954), p. 164.
 - [15] W. Bafford, J. M. F. Gunn, Physica C **156**, 515 (1988).
 - [16] V. I. Fesenko, V. N. Gorbunov, and V. P. Smilga, Physica C **176**, 551 (1991).
 - [17] R. Khasanov *et al.*, J. Phys. Condensed Matter **15**, L17 (2003).
 - [18] C. Panagopoulos, J. R. Cooper, and T. Xiang, Phys. Rev. B **57**, 13422 (1998).
 - [19] C. Panagopoulos, J. R. Cooper, T. Xiang, Y. S. Wang, and C. W. Chu, Phys. Rev. B **61**, 3808 (2000).
 - [20] T. Jacobs, S. Sridhar, Q. Li, G. D. Gu, and N. Koshizuka, Phys. Rev. Lett. **75**, 4516 (1995).
 - [21] K. D. Osborn *et al.*, cond-mat/0204417.
 - [22] M. E. Fisher and M. N. Barber, Phys. Rev. Lett. **28**, 1516 (1972).
 - [23] P. C. Hohenberg, A. Aharony, B. I. Halperin, and E. P. Siggia, Phys. Rev. B **13**, 2986 (1976).
 - [24] T. Schneider, cond-mat/0302024.
 - [25] J.-H. Chung *et al.*, Phys. Rev. B **67**, 014517 (2003)
 - [26] T. Schneider, cond-mat/0210697.
 - [27] T. Schneider, Europhys. Lett. **60**, 141 (2002).
 - [28] T. Schneider, Physica B **326**, 289 (2003).